Developmental Cognitive Neuroscience 50 (2021) 100968

Contents lists available at ScienceDirect

Developmental Cognitive Neuroscience

journal homepage: www.elsevier.com/locate/dcn

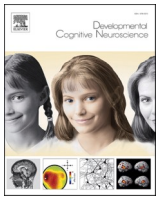

Sexually dimorphic development in the cortical oscillatory dynamics serving early visual processing

Madison H. Fung [a], Brittany K. Taylor [a], Brandon J. Lew [a,b], Michaela R. Frenzel [a], Jacob A. Eastman [a], Yu-Ping Wang [c], Vince D. Calhoun [d], Julia M. Stephen [e], Tony W. Wilson [a,*]

[a] Institute for Human Neuroscience, Boys Town National Research Hospital, Omaha, NE, USA
[b] College of Medicine, University of Nebraska Medical Center, Omaha, NE, USA
[c] Department of Biomedical Engineering, Tulane University, New Orleans, LA, USA
[d] Tri-institutional Center for Translational Research in Neuroimaging and Data Science (TReNDS) [Georgia State University, Georgia Institute of Technology, Emory University], Atlanta, GA, USA
[e] Mind Research Network, Albuquerque, NM, USA

ARTICLE INFO

Keywords:
Gamma
Alpha
Magnetoencephalography
Development
Vision

ABSTRACT

Successful interaction with one's visual environment is paramount to developing and performing many basic and complex mental functions. Although major aspects of visual development are completed at an early age, other structural and functional components of visual processing appear to be dynamically changing across a much more protracted period extending into late childhood and adolescence. However, the underlying neurophysiological changes and cortical oscillatory dynamics that support maturation of the visual system during this developmental period remain poorly understood. The present study utilized magnetoencephalography (MEG) to investigate maturational changes in the neural dynamics serving basic visual processing during childhood and adolescence (ages 9–15, n = 69). Our key results included robust sex differences in alpha oscillatory activity within the left posterior parietal cortex, and sex-by-age interactions in gamma activity in the right lingual gyrus and superior parietal lobule. Hierarchical regression revealed that the peak frequency of both the alpha and gamma responses predicted response power in parietal regions above and beyond the noted effects of age and sex. These findings affirm the view that neural oscillations supporting visual processing develop over a much more protracted period, and illustrate that these maturational trajectories are influenced by numerous elements, including age, sex, and individual variation.

1. Introduction

During childhood and adolescence, the human brain undergoes immense developmental changes in structure and function, ultimately shaping behavior. Successful interaction with one's visual environment is paramount to developing and performing many cognitive functions that are known to mature during this period. Although primary sensory cortices are thought to mature relatively early (Gogtay et al., 2004), structural and functional components of visual processing networks are still dynamically changing throughout late childhood and adolescence. Broadly, the overall pattern of cortical development produces linear white matter and non-linear grey matter changes that coincide with vast synaptic reorganization, extending to the cortical regions that underlie visual neural circuits (De Bellis et al., 2001; Giedd et al., 1999; Gogtay et al., 2004; Huttenlocher et al., 1982; Shaw et al., 2008; Wierenga et al., 2014). These structural developmental changes accompany functional and behavioral changes in several basic visual perception and processing domains, such as visual acuity and contrast sensitivity, which behaviorally do not exhibit fully mature patterns until later childhood and adolescence (Beazley et al., 1980; Kovács et al., 1999; Leat et al., 2009). Sex differences also become more apparent during this late developmental period, aligning with the sex-specific physiological changes occurring during puberty (Sisk and Foster, 2004). These pubertal changes could contribute to the development of the sexually dimorphic visual processing abilities present in adulthood (Shaqiri et al., 2018), though sex differences in visual-spatial abilities are also evident in pre-pubescent children (Kerns and Berenbaum, 1991).

Maturation of neural activity serving higher-order cognitive

* Corresponding author at: Institute for Human Neuroscience 378 Bucher Drive, Omaha, NE, 68010, USA.
E-mail address: tony.wilson@boystown.org (T.W. Wilson).

https://doi.org/10.1016/j.dcn.2021.100968
Received 19 December 2020; Received in revised form 2 April 2021; Accepted 25 May 2021
Available online 26 May 2021

processing during adolescence has been extensively studied using fMRI (for review, see Casey et al., 2005; Rubia, 2013), and studies have identified sex-specific developmental patterns of cortical network activity during complex visuospatial processing tasks in youth, such as mental rotation and spatial working memory (Hugdahl et al., 2006; Kucian et al., 2007; Schweinsburg et al., 2005). There is also a growing wealth of knowledge regarding changes in childhood neural oscillatory dynamics serving motor control (Gaetz et al., 2010; Heinrichs-Graham et al., 2018, 2020; Trevarrow et al., 2019; Wilson et al., 2010), higher-order cognition (Embury et al., 2019; Taylor et al., 2020; 2021), and more complex visuospatial attention (Fung et al., 2020; Killanin et al., 2020). Executing these tasks obviously requires input and integration of basic sensory information for successful performance. However, far less work has been done at earlier stages of the visual system to identify whether protracted development of neural oscillatory responses within these regions may occur in parallel and/or influence the higher-order developmental effects (Clements-Stephens et al., 2009). Of note, the neurotransmitter systems that support these population-level oscillatory responses continue to mature into adulthood (Hashimoto et al., 2009; Kilb, 2012; Uhlhaas et al., 2009, 2010), and this has a protracted impact on the evolving dynamics in these cortical circuits. For example, the neural oscillatory dynamics underlying visuospatial processing are known to be modulated by age across the adult lifespan and to differ by sex (Wiesman and Wilson, 2019), but many of these changes first emerge in childhood and continue throughout adolescence (Fung et al., 2020; Killanin et al., 2020). Other parameters of these oscillatory responses are also modulated by development. For example, the peak frequency of a given oscillatory response has been shown to vary by sex and decrease with age across the lifespan (Gaetz et al., 2012; Klimesch, 1999; van Pelt et al., 2018), with some evidence suggesting a degree of genetic heritability in mature peak/dominant frequencies (van Beijsterveldt and van Baal, 2002; van Pelt et al., 2012; Smit et al., 2006). Therefore, multiple parameters of visual processing dynamics continue to change during this late developmental period.

The main oscillatory responses serving visual processing and perception have been widely characterized in adult populations, and commonly consist of spectro-temporal responses within the theta (4–8 Hz), alpha (8–14 Hz), and gamma (>30 Hz) frequency ranges. Within early occipital regions, synchronizations in the gamma band are thought to index information processing and the fine-scale encoding of visual stimulus features, while theta responses represent the initial detection of salient stimuli (Busch et al., 2004; Hoogenboom et al., 2006; Muthukumaraswamy and Singh, 2013; Tallon-Baudry et al., 1996). Conversely, alpha desynchronizations (i.e., power decreases) generally reflect engagement of task-related cortical regions, thereby supporting the subsequent processing of the visual stimulus within occipital cortices (Klimesch, 1999, 2012). As noted above, these studies have primarily focused on adult populations and consequently the neurophysiological development of basic sensory processing in youth remains less understood.

In the present study we probed the impact of age and sex on the developmental trajectory of the oscillatory dynamics serving basic visual processing in a sample of typically developing children and adolescents. During magnetoencephalography (MEG) recording (Wilson et al., 2016), participants completed a sensory detection task. The resulting neural responses were transformed into the time-frequency domain and imaged using a beamformer approach. Whole-brain voxel-wise statistical tests were computed to assess the impact of age, sex, and their interaction on the resultant neural oscillatory responses, as well as to probe additional neurophysiological features of the responses, such as peak frequency. We hypothesized that males and females would exhibit unique oscillatory response profiles and maturational trajectories due to the known presence of sexually dimorphic visual perceptual abilities in adulthood, and the sexually dimorphic nature of neurodevelopment during adolescence.

2. Materials and methods

2.1. Participants

Seventy-four typically developing children and adolescents ages 9–15 years completed a basic sensory detection task as part of the National Science Foundation-funded Developmental Chronnecto-Genomics (Dev-CoG) study (Stephen et al., 2021). All participants were recruited from the University of Nebraska Medical Center (UNMC) site. Exclusionary criteria, determined by parent report, included neurological or psychiatric disorder, attention-deficit/hyperactivity disorder (ADHD) or other disorders affecting brain function, history of head trauma, and general MEG/MRI exclusionary criteria such as the presence of metal implants, dental braces or permanent retainers, or other metallic or otherwise magnetic non-removable devices. All procedures were approved by the UNMC Institutional Review Board, and informed consent from the child's parent or legal guardian, as well as assent from the child, were obtained before proceeding with the study.

2.2. Procedure

2.2.1. Task paradigm

A simple sensory detection task was used to engage the visual processing circuitry in this study (Fig. 1; see Trevarrow et al., 2019). During this task, participants were told to fixate on a centrally presented crosshair. After a variable ISI (range: 2400–2600 ms), one of three stimuli was presented for 800 ms: a stationary visual grating stimulus, an auditory steady-state stimulus, or both. All stimuli were supra-threshold and easily detected. The visual stimuli consisted of a series of vertical, stationary, square-wave gratings (3 cycles per degree) that were presented on a semi-translucent screen at an approximate distance of 1.07 m using a Panasonic PT-D7700U-K model DLP projector

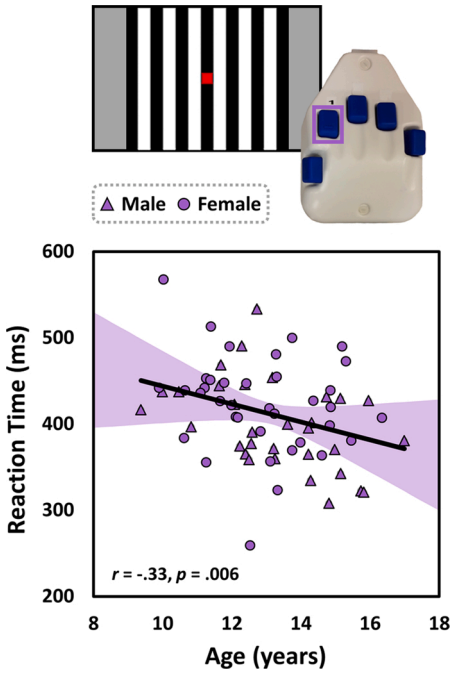

Fig. 1. The MEG visual processing task. Visual-only trials consisted of a fixation period lasting on average 2500 ms (2400–2600 ms variable ISI) including an 800 ms baseline period, followed by the appearance of the visual stimulus for 800 ms. The visual stimulus was a stationary black and white vertical grating. Participants pressed a button with their right index finger when the stimulus was detected. The scatterplot displays the negative correlation between age and reaction time, such that older children responded faster than their younger peers. Shaded bands represent 95 % confidence intervals.

with a refresh rate of 60 Hz and a contrast ratio of 4000:1. The gratings had a luminance contrast of 100 % (white bars alternating with black) and the ambient light in the room was low and held constant across the study. Participants were instructed to respond with a button press using their right index finger when any stimulus was detected. Each participant performed 300 trials (100 of each condition) in a pseudo-randomized order concurrent with MEG recording. Responses with a reaction time 2.5 SDs above or below the participant's mean were excluded from the final analyses. Of note, given our goals and hypotheses, the present study focused on the 100 visual-only trials to ensure homogenous brain responses.

2.2.2. MEG data acquisition

MEG recordings were conducted in a one-layer magnetically shielded room with active shielding engaged. Neuromagnetic responses were acquired with an Elekta/MEGIN MEG system with 306 magnetic sensors (204 planar gradiometers, 102 magnetometers; Elekta/MEGIN, Helsinki, Finland) using a bandwidth of 0.1–330 Hz, sampled continuously at 1 kHz. Each participant's data were individually corrected for head motion, and noise reduction was applied using the signal space separation method with a temporal extension (tSSS; Taulu et al., 2005; Taulu and Simola, 2006).

2.2.3. MEG coregistration and structural MRI processing

Preceding MEG measurement, four coils were attached to the participant's head and localized, together with the three fiducial points and scalp surface, using a 3-D digitizer (Fastrak 3SF0002, Polhemus Navigator Sciences, Colchester, VT, USA). Once the participant was positioned for MEG recording, an electric current with a unique frequency label (e.g., 322 Hz) was fed to each of the coils. This induced a measurable magnetic field and allowed each coil to be localized in reference to the MEG sensors throughout the recording session. Since coil locations were also known in head coordinates, all MEG measurements could be transformed into a common coordinate system. With this coordinate system, each participant's MEG data were coregistered with their individual structural T1-weighted MRI data prior to source space analyses using BESA MRI (Version 2.0). Structural T1-weighted MRI images were acquired using a Siemens Skyra 3T MRI scanner with a 32-channel head coil and a MP-RAGE sequence with the following parameters: TR = 2400 ms; TE = 1.94 ms; flip angle = 8°; FOV = 256 mm; slice thickness = 1 mm (no gap); voxel size = 1 × 1 × 1 mm. These data were aligned parallel to the anterior and posterior commissures and transformed into standardized space. Following source reconstruction (i.e., beamforming), each participant's 4.0 × 4.0 × 4.0 mm functional images were also transformed into standardized space using the transform that was previously applied to the structural MRI volume and spatially resampled.

2.2.4. MEG time-frequency transformation and statistics

Cardiac and ocular artifacts were removed from the data using signal-space projection (SSP), which was accounted for during source reconstruction (Uusitalo and Ilmoniemi, 1997). The continuous magnetic time series was divided into epochs of 2000 ms duration, including a baseline that extended from -850 to 50 ms before stimulus onset. Epochs containing artifacts (e.g., eye blinks, muscle artifacts, eye saccades, swallowing, coughing) were rejected based on a fixed-threshold method, supplemented with visual inspection. Briefly, the distribution of amplitude and gradient values per participant were computed using all trials, and the highest amplitude/gradient trials relative to the total distribution were excluded by selecting a threshold that rejected extreme values. Notably, thresholds were set independently for each participant due to differences among individuals in head size and sensor proximity, which strongly affect MEG signal amplitude. After artifact rejection, an average of 83.5 (SD = 5.1) trials per participant were used for further analysis, and this number was not significantly correlated with chronological age ($r = 0.0028$, $p = .982$) and did not differ by sex ($t = -.19$, $p = .851$).

Artifact-free epochs were transformed into the time-frequency domain using complex demodulation (resolution: 2.0 Hz, 25 ms; Papp and Ktonas, 1977; Kovach and Gander, 2016), and the resulting spectral power estimations per sensor were averaged over trials to generate time-frequency plots of mean spectral density. These sensor-level data were normalized using the respective bin's baseline power, which was calculated as the mean power during the -850 to -50 ms time period. The specific time-frequency windows used for imaging were determined by statistical analysis of the sensor-level spectrograms across the entire array of gradiometers. To reduce the risk of false-positive results while maintaining reasonable sensitivity, a two-stage procedure was followed to control for Type 1 error. In the first stage, two-tailed paired-sample t-tests against baseline were conducted on each data point, and the output spectrograms of t-values were thresholded at $p < .05$ to define time-frequency bins containing potentially significant oscillatory deviations across all participants. In stage two, the time-frequency bins that survived the threshold were clustered with temporally and/or spectrally neighboring bins that were also below the $p < .05$ threshold, and a cluster value was derived by summing all the t-values of all data points in the cluster. Nonparametric permutation testing was then used to derive a distribution of cluster values and the significance level of the observed clusters (from stage one) was tested directly using this distribution (Ernst, 2004; Maris and Oostenveld, 2007). For each comparison, 1000 permutations were computed to build a distribution of cluster values. Based on these analyses, the time-frequency windows that contained significant oscillatory events across all participants were subjected to a beamforming analysis (see Results). Of note, time-frequency clusters that occurred later than the mean reaction time across all participants were not considered in further analyses, as the aims of the study were to focus on visual processing rather than other processes involved in task completion (e.g., motor initiation, response/error-checking, etc.).

2.2.5. MEG source imaging, statistics, and virtual sensor analyses

Cortical responses were imaged through an extension of the linearly constrained minimum variance vector beamformer (Gross et al., 2001; Hillebrand et al., 2005; Van Veen et al., 1997), which employs spatial filters in the time-frequency domain to calculate source power for the entire brain volume. The single images are derived from the cross-spectral densities of all combinations of MEG gradiometers averaged over the time-frequency range of interest, and the solution of the forward problem for each location on a grid specified by input voxel space. Following convention, we computed noise-normalized, source power per voxel in each participant using active (i.e., task) and passive (i.e., baseline) periods of equal duration and bandwidth (Hillebrand et al., 2005). Such images are typically referred to as pseudo-t maps, with units (i.e., pseudo-t) that reflect noise-normalized power differences (i.e., active vs. passive) per voxel. MEG preprocessing and imaging used the BESA (V 6.1) software. Further details about our MEG data processing pipeline are available in a recent publication (Wiesman and Wilson, 2020).

Normalized differential source power was computed for the statistically-selected time-frequency bands (see below) over the entire brain volume per participant at 4.0 × 4.0 × 4.0 mm resolution. The resulting 3D maps of brain activity were then averaged across participants to assess the neuroanatomical basis of the significant oscillatory responses identified through the sensor-level analysis. Next, statistical analyses were computed on these oscillatory responses using SPM12 (Statistic Parametric Mapping (SPM), Wellcome Trust Center for Neuroimaging, http://www.fil.ion.ucl.ac.uk/spm/) running in MATLAB (2018b; MathWorks, Natick, Massachusetts, USA). Specifically, voxel-wise whole brain correlations between the participant-level maps and chronological age, and independent-samples t-tests between males and females were performed to probe the main effect of age and group effect of sex, respectively. One-way ANCOVAs were used to analyze the

interaction between age and sex in the development of these oscillatory responses. All statistical maps were corrected for multiple comparisons using the voxel-level family-wise error (FWE) method with a corrected significance of $p < .05$.

For each significant peak voxel identified from these whole-brain statistical maps, virtual sensor data were extracted, which corresponded to bilateral superior parietal and right lingual gyri. To create the virtual sensors, we applied the sensor weighting matrix derived through the forward computation to the preprocessed signal vector, which yielded two time series for each coordinate in source space, and then computed the vector sum of the two orientations ultimately yielding one time series per voxel per participant to be used for our analyses (Cheyne et al., 2006). Of note, these virtual sensor data were retransformed with a resolution of 1.0 Hz and 50 ms to provide more precise frequency values per participant while still preserving the same temporal windows used in the beamforming analysis. Once these virtual sensors were extracted, the characteristics of each response were assessed by correlating the peak frequency of each time-frequency component with age and sex, with Bonferroni corrections for multiple comparisons ($\alpha = .025$).

2.2.6. Hierarchical regression

Follow-up hierarchical regression analysis was conducted to examine the relationships between age, sex, peak frequency, and oscillatory power of significant responses identified in the whole-brain statistical maps. For each of these peak voxels, the pseudo-t value (i.e., normalized power) extracted from the peak voxels was regressed onto age, sex, and/or their interaction in the first step of the model. Age was grand mean centered. In the second step of the model, peak frequency measured within the voxel of interest was added as a predictor to further probe neurophysiological changes occurring in visual processing dynamics during this late developmental period.

3. Results

3.1. Demographic and behavioral results

Of the 74 participants who completed the task, five were excluded due to excessively noisy MEG data or other errors in MEG data acquisition. Thus, the final sample consisted of 69 children and adolescents ($M_{age} = 13.05$ years, $SD = 1.74$), with 37 females ($M_{age} = 12.83$ years, $SD = 1.66$) and 32 males ($M_{age} = 13.29$ years, $SD = 1.83$).

Participants performed well on the visual processing task, responding to 97.03 ± 3.97 % of trials with an average reaction time of 395.25 ± 55.10 ms. There was a significant negative correlation between age and reaction time ($r = -0.33$, $p = .006$; Fig. 1), such that older participants had faster reaction times than their younger peers, which did not vary between males and females.

3.2. Neural oscillatory responses to the task

Statistical analysis of the time-frequency spectrograms showed significant oscillatory responses in three distinct time-frequency windows (all $ps < .001$ after cluster-based permutation testing; Fig. 2). These included a significant increase from baseline (i.e., synchronization) in the gamma frequency range (60–72 Hz) from 50–300 ms after stimulus onset across posterior occipital sensors. Additionally, significant decreases from baseline (i.e., desynchronizations) in the alpha frequency (8–14 Hz) occurred from 250–500 ms over posterior sensors, and a significant desynchronization in the beta range (18–26 Hz) from 250–500 ms was identified in sensors near the sensorimotor cortex. These three significant oscillatory responses were imaged using a beamformer, and the resulting maps were grand-averaged per oscillatory response. Both the alpha and gamma responses were strongest bilaterally over the occipital cortices, while beta activity was tightly

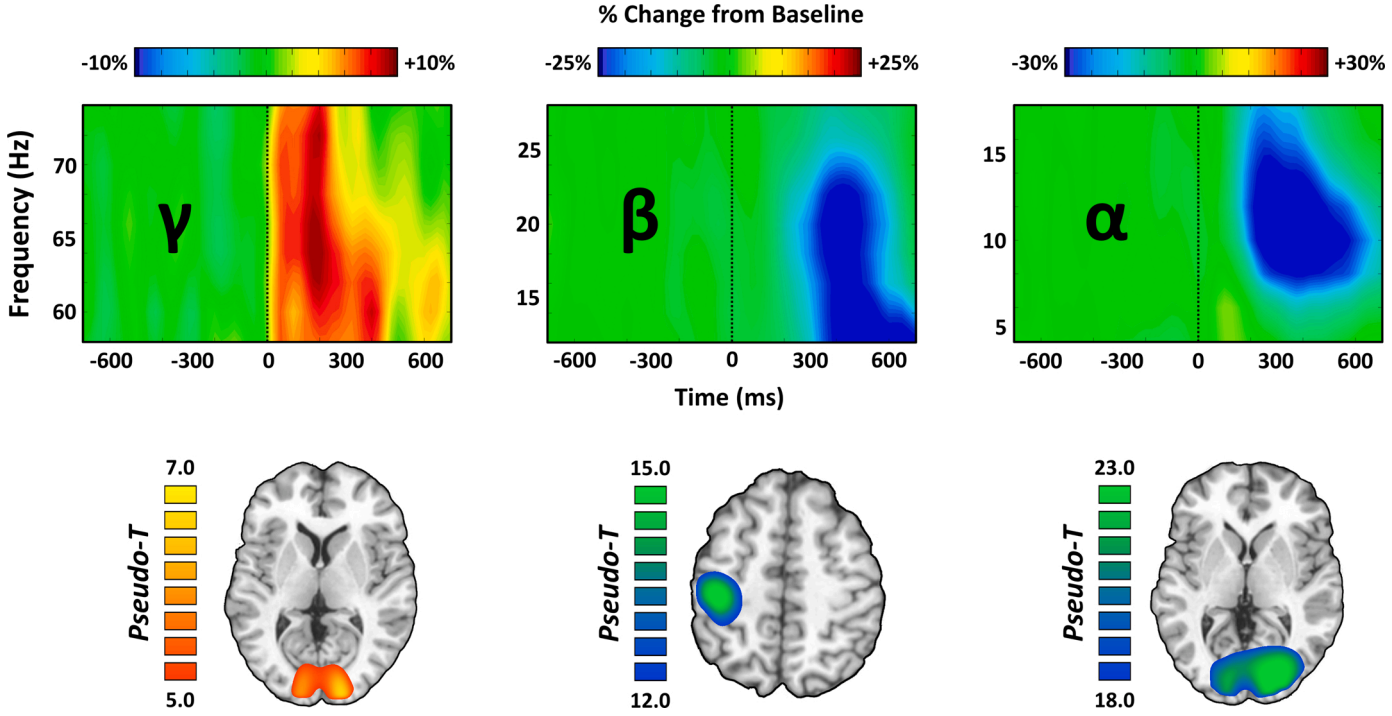

Fig. 2. (*Top*) Time-frequency spectrograms of significant oscillatory responses during the task. Data are from representative sensors: two posterior sensors (gamma: M2112, alpha: M2122) and one sensor near the left parietal cortex (beta: M0443). Warm colors represent power increases relative to the baseline, and cool colors reflect decreases in power relative to baseline. Time-frequency windows for source imaging (beamforming) were derived from statistical analyses of all sensor-level spectrograms, which indicated significant bins in alpha, beta, and gamma activity. (*Bottom*) Group-averaged beamformer images of each time-frequency window of interest across all participants. Alpha and gamma oscillatory responses were strongest in the bilateral occipital cortices, while beta was centered on the motor cortex and thus not further examined. Warm colors indicate synchronizations; cool colors indicate desynchronizations. Color scale bars indicate the strength of responses (pseudo-t). Brain images are displayed in neurological convention.

clustered on the contralateral primary motor cortex (Fig. 2). Since the beta activity was clearly indicative of the motor response (i.e., button press) and not related to visual perception or processing, we did not further examine this oscillatory component.

3.3. Sex effects on neural oscillatory activity

Independent samples t-tests on the whole-brain maps were performed to identify sex differences for the alpha and gamma oscillatory responses. We found significant sex differences in alpha oscillatory activity within the left superior parietal lobule, such that females showed stronger desynchronizations relative to males ($t = 4.44$, $p_{FWE} = .027$; Fig. 3). Of note, there were no significant sex differences in gamma activity.

3.4. Age effects on neural oscillatory activity

Developmental effects on neural oscillatory activity were examined by correlating each participant's functional map, per alpha and gamma oscillatory component, with their chronological age. There were no significant correlations between age and oscillatory activity in the alpha or gamma bands that met our conservative threshold ($p_{FWE} < .05$).

3.5. Sex by age interactions in neural oscillatory activity

We examined whether developmental changes in oscillatory activity varied by sex as a function of age. For these analyses, we performed whole-brain one-way ANCOVAs with sex as the factor and age as the covariate within each significant oscillatory window. These analyses revealed two significant clusters within the gamma range; females showed stronger gamma activity with increasing age within the right superior parietal lobule ($t = 4.54$, $p_{FWE} = .035$; Fig. 4) and the right lingual gyrus ($t = 4.43$, $p_{FWE} = .046$; Fig. 5), whereas males showed the opposite pattern as a function of age. There were no significant sex-by-age interactions within the alpha range.

3.6. Virtual sensor analyses and statistics

Virtual sensor data were extracted from the peak voxels within each significant cluster to examine whether individual peak frequencies within these regions also modulated developmental changes in oscillatory activity. Hierarchical regression analyses were then conducted to probe more complex statistical relationships between oscillatory activity, sex, age, and peak frequency. For the alpha band sex difference observed in the left superior parietal region, response power was regressed onto sex in the first step of the model and onto individual alpha frequency (IAF; i.e., peak frequency of the alpha response) for the second step. The overall model accounted for 38 % of the variance in alpha response power ($F(262) = 18.36$, $p = .001$; Table 1), with the IAF accounting for a significant amount of variance in alpha response power above and beyond the effect of sex ($\Delta R^2 = .13$, $F(160) = 12.98$, $p = .001$, $\beta = 0.37$, $b = 2.53$, CI [1.13, 3.94]).

Similarly, hierarchical regression analyses were performed on the two age-by-sex interaction peaks (i.e., right superior parietal and right lingual gyrus) observed in the whole-brain ANCOVA maps. Sex, age, and the age-by-sex interaction were entered in the first step of the model, and peak gamma frequency (PGF) measured within the respective peak of each region was entered into the second step. For the superior parietal peak, the overall model accounted for 38 % of the variance ($F(457) = 8.12$, $p < .001$; Table 2), with PGF significantly contributing to the variance explained above and beyond the effects of age, sex, and their interaction ($\Delta R^2 = .09$, $F(153) = 7.70$, $p = .008$, $\beta = -0.31$, $b = -0.09$). Of note, the PGF in the lingual gyrus did not significantly predict response power above and beyond the effects of age and sex ($\Delta R^2 = .02$, $F(153) = 1.39$, $p = .244$, $\beta = -0.15$, $b = -0.08$).

Finally, prior to conducting our hierarchical regressions, we examined correlations between the peak frequency indices, age, and sex to determine whether we should include any additional terms in the

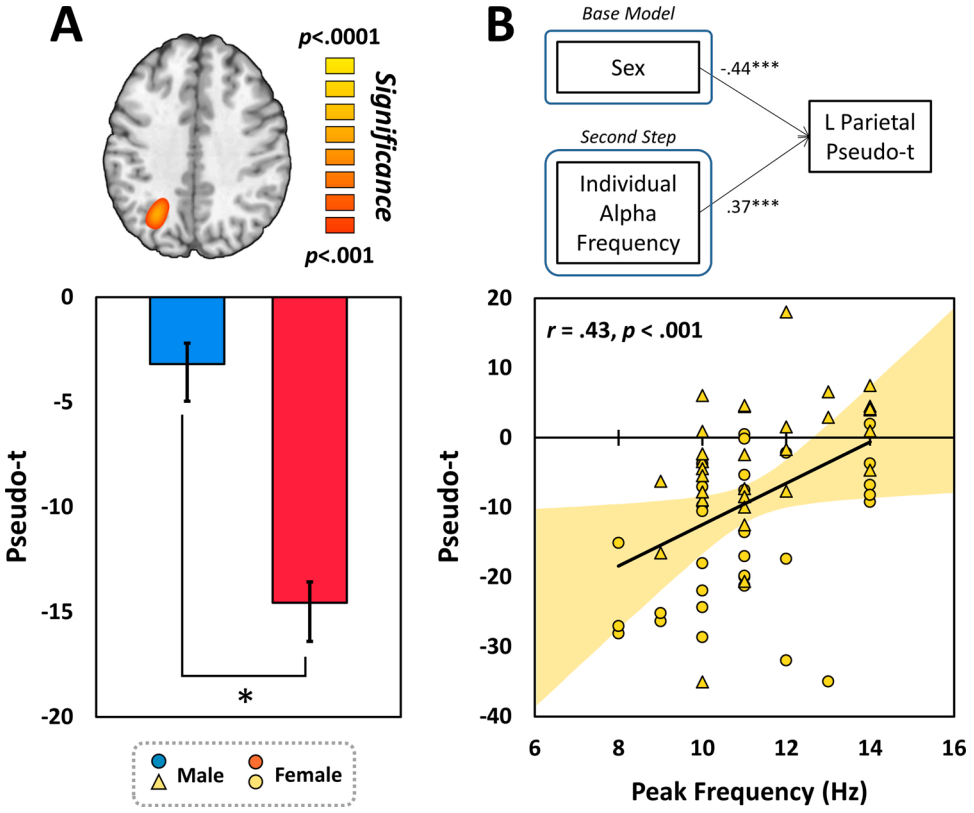

Fig. 3. Sex Effect in Visual Alpha Activity. (A) Whole-brain independent-samples *t*-test showed significant sex differences in alpha oscillatory activity within the left superior parietal lobule, such that females showed stronger alpha decreases (i.e., desynchronizations) relative to males ($p_{FWE} = .027$). The brain image is displayed following neurological convention. Bar graph showing the group mean sex difference in response power at the peak voxel. (B) Graphical representation of the hierarchical regression, with standardized coefficients, shows that sex and individual alpha peak frequency both significantly predicted alpha response power. Scatterplot displays the relationship between peak alpha frequency and response power, in which lower individual alpha peak frequency was associated with stronger alpha desynchronization (i.e. more negative response power). Thus, within the whole sample, individual alpha frequency predicts pseudo-t response power above and beyond the effect of sex entered in the base model. Shaded bands represent 95 % confidence intervals. *** $p < .001$, ** $p < .01$, * $p < .05$.

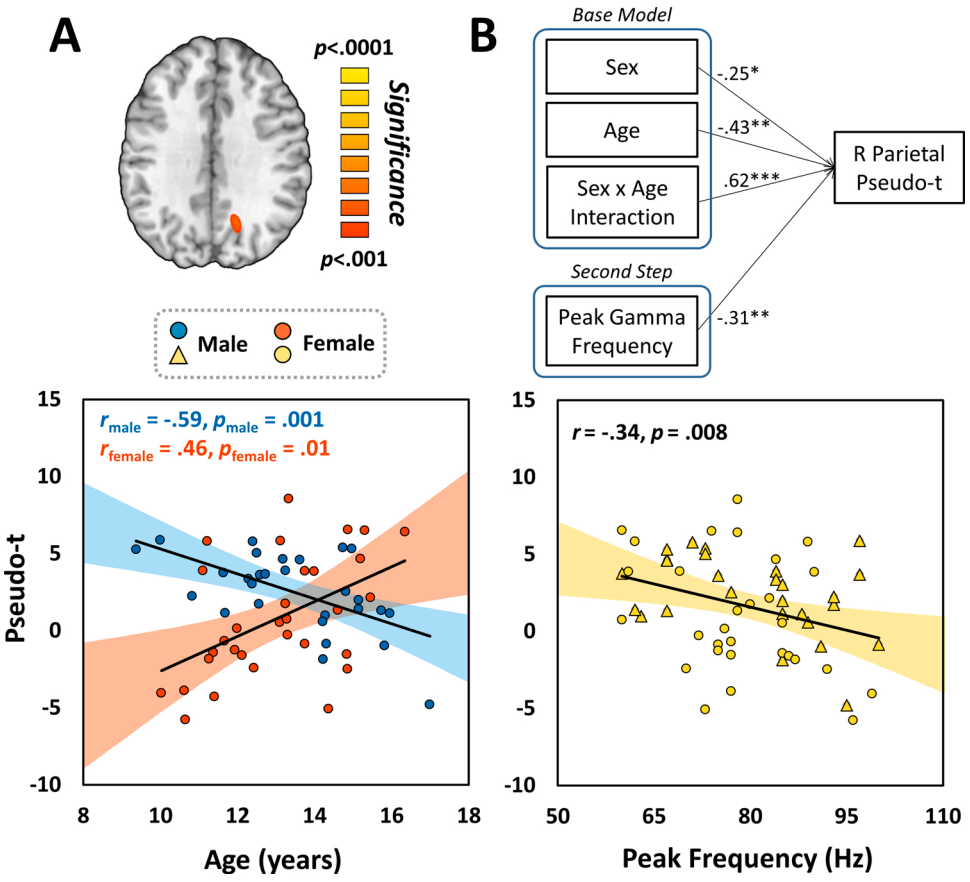

Fig. 4. Sex by Age Interactions in Visual Gamma Activity in the Right Superior Parietal Lobule. (A) Whole-brain statistical map showing this sex difference as a function of age in the right superior parietal lobule (p_{FWE} = .035). The brain image is displayed following neurological convention. Scatterplot showing the significant age-by-sex interaction in gamma response amplitude. Shaded bands represent 95 % confidence intervals. (B) Graphical representation of the hierarchical regression model, with standardized coefficients, showing that the peak gamma frequency of the response significantly predicts pseudo-t response power above and beyond the effects of age, sex, and the sex-by-age interaction entered in the base model. Scatterplot showing significant inverse relationship between individual peak gamma frequency and gamma response strength above and beyond the effects of age, sex, and the sex-by-age interaction entered in the base model within the whole sample. Shaded bands represent 95 % confidence intervals. *** $p < .001$, ** $p < .01$, * $p < .05$.

hierarchical models. However, we found no significant correlations between peak frequency and age or sex after controlling for multiple comparisons ($rs = -0.27$ to 0.15).

4. Discussion

The present study examined the effects of age and sex on the dynamics of basic visual processing in a sample of typically developing youth. Behaviorally, reaction time was negatively correlated with age, such that older children responded to the visual stimulus faster than their younger peers. In regard to the neural dynamics serving task performance, we observed robust increases in power (i.e., neural synchronizations) in the gamma (60–72 Hz) range, and decreases in power (i.e., desynchronizations) in the alpha band (8–14 Hz), both of which were strongest in the occipital cortices. Further, whole-brain statistical tests showed these oscillatory responses uniquely interacted with age and sex in the parietal and ventral association cortices, and the peak frequency of these responses additionally predicted neural response power. These findings illuminate the unique, sexually dimorphic trajectories and complex interactions involved in the development of the neural oscillations underlying basic aspects of visual function in late childhood and adolescence.

One of our main findings was the age-by-sex interaction in the gamma band response, which involved key regions serving visual processing, including the right lingual gyrus and the right superior parietal lobule. Females showed stronger gamma activity with increasing chronological age in these areas, while males showed the opposite pattern, exhibiting weaker gamma activity across development. In general, coordination among neural populations continues to mature into adulthood, with visual gamma activity serving fine-scale processing and increasing in synchrony throughout this developmental period (Uhlhaas et al., 2010; Werkle-Bergner et al., 2009). Prior literature has shown that males and females exhibit differences in visual perception in adulthood, for example, in measures of contrast sensitivity and visual acuity (Shaqiri et al., 2018), and these functions are not mature until later in adolescence (Beazley et al., 1980; Kovács et al., 1999; Leat et al., 2009). Thus, the current results may illustrate the emergence of these sexually dimorphic trajectories for specific stimulus parameters. These sex-specific maturational trajectories during childhood likely develop into differential patterns of cortical activity for processing the same basic visual stimuli in adulthood; as a result, females may utilize these ancillary visual areas more broadly, whereas males may exhibit less activity in these regions. Alternatively, increased activity in these higher visual areas could indicate a difference in processing strategies, more effortful processing, or more consistent responses in females, all of which could underlie these sexually dimorphic changes in oscillatory power. Future work is needed to distinguish the specific mechanism underlying these differences.

The sex-specific maturation trajectories in gamma and alpha activity may also index differences in higher-order attentional modulation between males and females. Of note, superior parietal cortical regions are implicated in the basic detection of sensory stimuli and visuospatial attention (Bushara et al., 1999) and gamma activity is also modulated by attention allocation (Doesburg et al., 2008; Edden et al., 2009; Tallon-Baudry et al., 1996; Vidal et al., 2006). Thus, these sex-specific maturation trajectories may index the development of higher-order attentional modulation in females. In addition to the noted effects of age and sex on gamma responses, cortical alpha activity in the left posterior parietal cortex varied by sex, such that females showed markedly stronger desynchronizations than males. The classic alpha event-related desynchronization generally reflects cortical activation of task-related brain regions, with task irrelevant regions often exhibiting either an alpha synchronization or a smaller desynchronization (Klimesch, 1999, 2012). The sexually dimorphic alpha responses identified

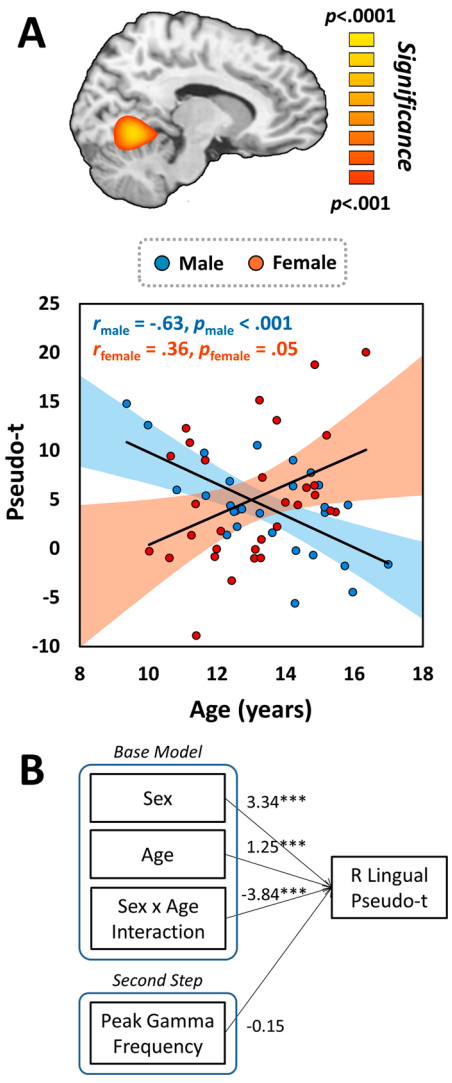

Fig. 5. Sex by Age Interactions in Visual Gamma Activity in the Right Lingual Gyrus. (A) The whole-brain statistical map shows this sex difference as a function of age in the right lingual gyrus. Scatterplot showing the significant age-by-sex interaction in gamma response amplitude within the right lingual gyrus. Shaded bands represent 95 % confidence intervals. (B) Graphical representation of the hierarchical regression model, with standardized coefficients, showing that the peak gamma frequency of the response *does not* significantly predict pseudo-t response power above and beyond the effects of age, sex, and the sex-by-age interaction entered in the base model. *** $p < .001$, ** $p < .01$, * $p < .05$.

in the present study again demonstrate female-specific recruitment of parietal association areas often involved in attention and higher-order processing, though unlike the gamma band results, these sex differences did not vary with age. Alpha activity has been documented to vary by age and sex during verbal working memory processing (Embury et al., 2019); however, most MEG studies of cognitive development have observed these interactions in other frequency bands (Fung et al., 2020; Killanin et al., 2020; Taylor et al., 2020). Future studies could utilize different visual stimuli or include further attentional manipulations to determine the extent to which alpha activity during basic visual perception exhibits developmental alterations, or whether such maturational effects are limited to more complex tasks and other oscillatory responses.

Importantly, the peak frequency of the alpha and the gamma band responses each predicted response power above and beyond the noted effects of age and sex. Broadly, task-related peak gamma frequency and individual alpha frequency have been documented to change throughout the lifespan and vary by sex (Gaetz et al., 2012; Klimesch, 1999; van Pelt et al., 2018). Though peak frequencies in the present study did not independently exhibit sex or developmental effects, individual alpha frequency and peak gamma frequency both significantly predicted response power in the posterior parietal regions above and beyond the developmental effects of age and sex. These unique effects of peak frequency on brain activity emphasize the multifaceted individual differences that contribute to shaping the trajectory of brain maturation, including potentially heritable influences. Prior literature has shown that the degree of genetic influence on the maturation of brain structure and function varies by brain region throughout development. Specifically, earlier maturing regions (e.g., motor and sensory cortices) exhibit more heritable patterns of structural change earlier in development, while other higher-order association regions that mature later in development show more heritability at older ages (Lenroot et al., 2009; van Soelen et al., 2012). Since individual peak frequencies of oscillatory responses have been shown to be highly heritable (Smit et al., 2006; van Beijsterveldt and van Baal, 2002; van Pelt et al., 2012), the present findings of peak frequency uniquely shaping response power could shed further light on potential genetic influences that modulate neurophysiological maturation in youth. Interestingly, the impact of peak frequency on response power was only significant in the bilateral parietal areas, which as previously discussed, are frequently implicated in attentional and higher-order cognitive and perceptual processing. This distinction could further parallel the preferentially delayed heritable influence on functional cortical development in higher-order association areas, relative to other basic sensory regions that structurally mature earlier in development and show less genetic influence with more maturation. Thus, these findings provide a more comprehensive view of the development of neural oscillatory activity, where age and sex, in addition to potentially heritable and/or individual differences in peak frequency concurrently contribute to the functional maturation of these neurophysiological responses during a protracted developmental period.

Integrating the present findings into the broader context of adolescent development can help to shed light on the nuances of neurophysiological maturation. It is well documented throughout the literature that cognitive, social, and emotional functions dramatically change throughout adolescence, consisting of substantial behavioral and functional maturation (Blakemore, 2012; Casey et al., 2005; Luna et al.,

Table 1
Hierarchical Multiple Regression Results for Alpha Response Power.

Model	*b*	*SE*	*t*	β	*F*	R^2	ΔF	ΔR^2	95 % CI
First Step:									
(Constant)	−3.19	1.82	−1.75		19.84***	0.25			(−6.82, 0.45)
Sex	−11.36	2.55	−4.46***	−0.50					(−16.47, −6.26)
Second Step:									
(Constant)	−32.10	8.20	−3.92***		18.36***	0.38	12.98***	0.13	(−48.49, −15.70)
Sex	−10.14	2.36	−4.30***	−0.44					(−14.86, −5.43)
IAF	2.53	0.70	3.60**	0.37					(1.13, 3.94)

*** $p < .001$, ** $p < .01$, * $p < .05$.
Sex Coding: Female = 1, Male = 0; IAF = Individual Alpha Frequency.

Table 2
Hierarchical Multiple Regression Results for Gamma Response Power.

Model: Sup. Parietal	*b*	*SE*	*t*	β	*F*	R^2	Δ*F*	ΔR^2	95 % CI
First Step:									
(Constant)	2.66	0.55	4.81***		7.34***	0.29			(1.55, 3.76)
Sex	−1.48	0.77	−1.93***	−0.22					(−3.02, 0.06)
Age	−0.81	0.30	−2.69***	−0.43					(−1.42, −0.21)
Interaction	1.87	0.44	4.24***	0.67					(0.99, 2.76)
Second Step:									
(Constant)	10.10	2.73	3.70***		8.12***	0.38	7.70**	0.90	(4.62, 15.57)
Sex	−1.68	0.73	−2.30*	−0.25					(−3.14, −0.22)
Age	−0.82	0.29	−2.87**	−0.43					(−1.39, −0.25)
Interaction	1.72	0.42	4.10***	0.62					(0.88, 2.56)
PGF	−0.09	0.03	−2.78***	−0.31					(−0.16, −0.03)
Model: Lingual	***b***	***SE***	***T***	**β**	***F***	**R^2**	**Δ*F***	**ΔR^2**	**95 % CI**
First Step:									
(Constant)	4.53	0.94	4.81***		5.50***	0.23			(2.64, 6.41)
Sex	1.21	1.31	0.92**	0.11					(−1.42, 3.84)
Age	−1.62	0.52	−3.15**	−0.52					(−2.66, −0.59)
Interaction	2.92	0.75	3.88***	0.64					(1.41, 4.43)
Second Step:									
(Constant)	10.60	5.24	2.02*		4.50	0.25	1.39	0.02	(0.10, 21.10)
Sex	0.85	1.34	0.63	0.08					(−1.85, 3.54)
Age	−1.71	0.52	−3.29**	−0.55					(−2.75, −0.67)
Interaction	2.81	0.76	3.73***	0.61					(1.30, 4.34)
PGF	−0.08	0.07	−1.18	−0.15					(−0.21, 0.05)

*** $p < .001$, ** $p < .01$, * $p < .05$.
Sex Coding: Female = 1, Male = 0; PGF = Peak Gamma Frequency.

2004; Rubia, 2013). Executing these tasks requires input and integration of basic sensory information for successful performance; the extended evolution of basic visual processing dynamics observed in the present study provides evidence that changes in adolescence may be much more complex than previously thought. Essentially, if elements of early visual processing are still functionally maturing throughout late childhood and adolescence, these changes in basic sensory processing are likely in some part influencing the concomitant higher-level cognitive and affective maturational trajectories around the time of puberty. Since successfully performing most of these behaviors requires some level of basic visual input, the individual and developmental differences observed in the current study could underlie the changes in performance, strategy, and/or neural activity seen in numerous other domains more commonly associated with childhood and adolescent growth.

In conclusion, the present study examined the complex nature of the neurophysiological processes that are changing throughout the protracted period of adolescent development, even in regard to basic visual perception and sensory processing. Age, sex, and peak frequency all uniquely and differentially impacted oscillatory response power during early visual processing, which reflects the multitude of individual differences influencing neural oscillatory development throughout childhood and adolescence. Specifically, our findings highlight the protracted nature of functional brain development in which changes in basic visual processing are still occurring; this may be antecedent to or concurrent with other rapid and extensive cognitive, affective, and behavioral changes that also dramatically change during this maturational period.

Data availability

All data are available upon request to the corresponding author (TWW). Data will be made publicly available upon study completion.

Declaration of Competing Interest

The authors declare that they have no known competing financial interests or personal relationships that could have appeared to influence the work reported in this paper.

Acknowledgements

This research was supported by grants R01-MH121101 (TWW), R01-MH103220 (TWW), R01-MH116782 (TWW), R01-MH118013 (TWW), F30-DA048713 (BJL), and R01-EB020407 (VDC) from the National Institutes of Health, and grant #1539067 from the National Science Foundation (TWW, VCD, Y-PW, and JMS). The funders had no role in study design, data collection and analysis, decision to publish, or preparation of the manuscript.

References

Beazley, L.D., Illingworth, D.J., Jahn, A., Greer, D.V., 1980. Contrast sensitivity in children and adults. Br. J. Ophthalmol. 64 (11), 863–866.
Blakemore, S.J., 2012. Development of the social brain in adolescence. J. R. Soc. Med. 105 (3), 111–116.
Busch, N.A., Debener, S., Kranczioch, C., Engel, A.K., Herrmann, C.S., 2004. Size matters: effects of stimulus size, duration and eccentricity on the visual gamma-band response. Clin. Neurophysiol. 115 (8), 1810–1820.
Bushara, K.O., Weeks, R.A., Ishii, K., Catalan, M.J., Tian, B., Rauschecker, J.P., Hallett, M., 1999. Modality-specific frontal and parietal areas for auditory and visual spatial localization in humans. Nat. Neurosci. 2 (8), 759–766.
Casey, B.J., Tottenham, N., Liston, C., Durston, S., 2005. Imaging the developing brain: what have we learned about cognitive development? Trends Cogn. Sci. (Regul. Ed.) 9 (3), 104–110.
Cheyne, D., Bakhtazad, L., Gaetz, W., 2006. Spatiotemporal mapping of cortical activity accompanying voluntary movements using an event-related beamforming approach. Hum. Brain Mapp. 27 (3), 213–229.
Clements-Stephens, A.M., Rimrodt, S.L., Cutting, L.E., 2009. Developmental sex differences in basic visuospatial processing: differences in strategy use? Neurosci. Lett. 449 (3), 155–160.
De Bellis, M.D., Keshavan, M.S., Beers, S.R., Hall, J., Frustaci, K., Masalehdan, A., Noll, J., Boring, A.M., 2001. Sex differences in brain maturation during childhood and adolescence. Cereb. Cortex 11 (6), 552–557.
Doesburg, S.M., Roggeveen, A.B., Kitajo, K., Ward, L.M., 2008. Large-scale gamma-band phase synchronization and selective attention. Cereb. Cortex 18 (2), 386–396.
Edden, R.A., Muthukumaraswamy, S.D., Freeman, T.C., Singh, K.D., 2009. Orientation discrimination performance is predicted by GABA concentration and gamma oscillation frequency in human primary visual cortex. J. Neurosci. 29 (50), 15721–15726.
Embury, C.M., Wiesman, A.I., Proskovec, A.L., Mills, M.S., Heinrichs-Graham, E., Wang, Y.P., Calhoun, V.D., Stephen, J.M., Wilson, T.W., 2019. Neural dynamics of verbal working memory processing in children and adolescents. Neuroimage 185, 191–197.
Ernst, M.D., 2004. Permutation methods: a basis for exact inference. Stat. Sci.: Stat. Sci. 676–685.

Fung, M.H., Taylor, B.K., Frenzel, M.R., Eastman, J.A., Wang, Y.P., Calhoun, V.D., Stephen, J.M., Wilson, T.W., 2020. Pubertal testosterone tracks the developmental trajectory of neural oscillatory activity serving visuospatial processing. Cereb. Cortex 30 (11), 5960–5971.
Gaetz, W., Macdonald, M., Cheyne, D., Snead, O.C., 2010. Neuromagnetic imaging of movement-related cortical oscillations in children and adults: age predicts post-movement beta rebound. Neuroimage 51 (2), 792–807.
Gaetz, W., Roberts, T.P., Singh, K.D., Muthukumaraswamy, S.D., 2012. Functional and structural correlates of the aging brain: relating visual cortex (V1) gamma band responses to age-related structural change. Hum. Brain Mapp. 33 (9), 2035–2046.
Giedd, J.N., Blumenthal, J., Jeffries, N.O., Castellanos, F.X., Liu, H., Zijdenbos, A., Paus, T., Evans, A.C., Rapoport, J.L., 1999. Brain development during childhood and adolescence: a longitudinal MRI study. Nat. Neurosci. 2 (10), 861–863.
Gogtay, N., Giedd, J.N., Lusk, L., Hayashi, K.M., Greenstein, D., Vaituzis, A.C., Nugent, T. F., Herman, D.H., Clasen, L.S., Toga, A.W., et al., 2004. Dynamic mapping of human cortical development during childhood through early adulthood. Proc. Natl. Acad. Sci. U. S. A. 101 (21), 8174–8179.
Gross, J., Kujala, J., Hamalainen, M., Timmermann, L., Schnitzler, A., Salmelin, R., 2001. Dynamic imaging of coherent sources: studying neural interactions in the human brain. Proc. Natl. Acad. Sci. U. S. A. 98 (2), 694–699.
Hashimoto, T., Nguyen, Q.L., Rotaru, D., Keenan, T., Arion, D., Beneyto, M., Gonzalez-Burgos, G., Lewis, D.A., 2009. Protracted developmental trajectories of GABAA receptor alpha1 and alpha2 subunit expression in primate prefrontal cortex. Biol. Psychiatry 65 (12), 1015–1023.
Heinrichs-Graham, E., McDermott, T.J., Mills, M.S., Wiesman, A.I., Wang, Y.P., Stephen, J.M., Calhoun, V.D., Wilson, T.W., 2018. The lifespan trajectory of neural oscillatory activity in the motor system. Dev. Cogn. Neurosci. 30, 159–168.
Heinrichs-Graham, E., Taylor, B.K., Wang, Y.P., Stephen, J.M., Calhoun, V.D., Wilson, T. W., 2020. Parietal oscillatory dynamics mediate developmental improvement in motor performance. Cereb. Cortex.
Hillebrand, A., Singh, K.D., Holliday, I.E., Furlong, P.L., Barnes, G.R., 2005. A new approach to neuroimaging with magnetoencephalography. Hum. Brain Mapp. 25 (2), 199–211.
Hoogenboom, N., Schoffelen, J.M., Oostenveld, R., Parkes, L.M., Fries, P., 2006. Localizing human visual gamma-band activity in frequency, time and space. Neuroimage 29 (3), 764–773.
Hugdahl, K., Thomsen, T., Ersland, L., 2006. Sex differences in visuo-spatial processing: an fMRI study of mental rotation. Neuropsychologia 44 (9), 1575–1583.
Huttenlocher, P.R., de Courten, C., Garey, L.J., Van der Loos, H., 1982. Synaptogenesis in human visual cortex–evidence for synapse elimination during normal development. Neurosci. Lett. 33 (3), 247–252.
Kerns, K.A., Berenbaum, S.A., 1991. Sex differences in spatial ability in children. Behav. Genet. 21 (4), 383–396.
Kilb, W., 2012. Development of the GABAergic system from birth to adolescence. Neuroscientist 18 (6), 613–630.
Killanin, A.D., Wiesman, A.I., Heinrichs-Graham, E., Groff, B.R., Frenzel, M.R., Eastman, J.A., Wang, Y.P., Calhoun, V.D., Stephen, J.M., Wilson, T.W., 2020. Development and sex modulate visuospatial oscillatory dynamics in typically-developing children and adolescents. Neuroimage 221, 117192.
Klimesch, W., 1999. EEG alpha and theta oscillations reflect cognitive and memory performance: a review and analysis. Brain Res. Brain Res. Rev. 29 (2–3), 169–195.
Klimesch, W., 2012. α-band oscillations, attention, and controlled access to stored information. Trends Cogn. Sci. 16 (12), 606–617.
Kovach, C.K., Gander, P.E., 2016. The demodulated band transform. J. Neurosci. Methods 261, 135–154.
Kovács, I., Kozma, P., Fehér, A., Benedek, G., 1999. Late maturation of visual spatial integration in humans. Proc. Natl. Acad. Sci. U. S. A. 96 (21), 12204–12209.
Kucian, K., von Aster, M., Loenneker, T., Dietrich, T., Mast, F.W., Martin, E., 2007. Brain activation during mental rotation in school children and adults. J. Neural Transm. (Vienna) 114 (5), 675–686.
Leat, S.J., Yadav, N.K., Irving, E.L., 2009. Development of visual acuity and contrast sensitivity in children. J. Optom. 2 (1), 19–26.
Lenroot, R.K., Schmitt, J.E., Ordaz, S.J., Wallace, G.L., Neale, M.C., Lerch, J.P., Kendler, K.S., Evans, A.C., Giedd, J.N., 2009. Differences in genetic and environmental influences on the human cerebral cortex associated with development during childhood and adolescence. Hum. Brain Mapp. 30 (1), 163–174.
Luna, B., Garver, K.E., Urban, T.A., Lazar, N.A., Sweeney, J.A., 2004. Maturation of cognitive processes from late childhood to adulthood. Child Dev. 75 (5), 1357–1372.
Maris, E., Oostenveld, R., 2007. Nonparametric statistical testing of EEG- and MEG-data. J. Neurosci. Methods 164 (1), 177–190.
Muthukumaraswamy, S.D., Singh, K.D., 2013. Visual gamma oscillations: the effects of stimulus type, visual field coverage and stimulus motion on MEG and EEG recordings. Neuroimage 69, 223–230.
Papp, N., Ktonas, P., 1977. Critical evaluation of complex demodulation techniques for the quantification of bioelectrical activity. Biomed. Sci. Instrum. 13, 135–145.
Rubia, K., 2013. Functional brain imaging across development. Eur. Child Adolesc. Psychiatry 22 (12), 719–731.
Schweinsburg, A.D., Nagel, B.J., Tapert, S.F., 2005. fMRI reveals alteration of spatial working memory networks across adolescence. J. Int. Neuropsychol. Soc. 11 (5), 631–644.
Shaqiri, A., Roinishvili, M., Grzeczkowski, L., Chkonia, E., Pilz, K., Mohr, C., Brand, A., Kunchulia, M., Herzog, M.H., 2018. Sex-related differences in vision are heterogeneous. Sci. Rep. 8 (1), 7521.
Shaw, P., Kabani, N.J., Lerch, J.P., Eckstrand, K., Lenroot, R., Gogtay, N., Greenstein, D., Clasen, L., Evans, A., Rapoport, J.L., et al., 2008. Neurodevelopmental trajectories of the human cerebral cortex. J. Neurosci. 28 (14), 3586–3594.
Sisk, C.L., Foster, D.L., 2004. The neural basis of puberty and adolescence. Nat. Neurosci. 7 (10), 1040–1047.
Smit, C.M., Wright, M.J., Hansell, N.K., Geffen, G.M., Martin, N.G., 2006. Genetic variation of individual alpha frequency (IAF) and alpha power in a large adolescent twin sample. Int. J. Psychophysiol. 61 (2), 235–243.
Stephen, J.M., Solis, I., Janowwich, J., Stern, M., Frenzel, M.R., Eastman, J.A., Mills, M. S., Embury, C.M., Coolidge, N.M., Heinrichs-Graham, E., Mayer, A., Lui, J., Wang, Y. P., Wilson, T.W., Calhoun, V.D., 2021. The Developmental Chronnecto-Genomics (Dev-CoG) study: a multimodal study on the developing brain. Neuroimage 225, 117438.
Tallon-Baudry, C., Bertrand, O., Delpuech, C., Pernier, J., 1996. Stimulus specificity of phase-locked and non-phase-locked 40 Hz visual responses in human. J. Neurosci. 16 (13), 4240–4249.
Taulu, S., Simola, J., 2006. Spatiotemporal signal space separation method for rejecting nearby interference in MEG measurements. Phys. Med. Biol. 51 (7), 1759–1768.
Taulu, S., Juha, S., Kajola, M., 2005. Applications of the signal space separation method. IEEE Trans. Signal Process. 3359–3372.
Taylor, B.K., Eastman, J.A., Frenzel, M.R., Embury, C.M., Wang, Y.P., Calhoun, V.D., Stephen, J.M., Wilson, T.W., 2021. Neural oscillations underlying selective attention follow sexually divergent developmental trajectories during adolescence. Dev. Cogn. Neurosci. 49, 100961.
Taylor, B.K., Embury, C.M., Heinrichs-Graham, E., Frenzel, M.R., Eastman, J.A., Wiesman, A.I., Wang, Y., Calhoun, V.D., Stephen, J.M., Wilson, T.W., 2020. Neural oscillatory dynamics serving abstract reasoning reveal robust sex differences in typically-developing children and adolescents. Dev. Cogn. Neurosci. 42, 100770.
Trevarrow, M.P., Kurz, M.J., McDermott, T.J., Wiesman, A.I., Mills, M.S., Wang, Y.P., Calhoun, V.D., Stephen, J.M., Wilson, T.W., 2019. The developmental trajectory of sensorimotor cortical oscillations. Neuroimage 184, 455–461.
Uhlhaas, P.J., Roux, F., Singer, W., Haenschel, C., Sireteanu, R., Rodriguez, E., 2009. The development of neural synchrony reflects late maturation and restructuring of functional networks in humans. Proc. Natl. Acad. Sci. U. S. A. 106 (24), 9866–9871.
Uhlhaas, P.J., Roux, F., Rodriguez, E., Rotarska-Jagiela, A., Singer, W., 2010. Neural synchrony and the development of cortical networks. Trends Cogn. Sci. 14 (2), 72–80.
Uusitalo, M.A., Ilmoniemi, R.J., 1997. Signal-space projection method for separating MEG or EEG into components. Med. Biol. Eng. Comput. 35 (2), 135–140.
van Beijsterveldt, C.E., van Baal, G.C., 2002. Twin and family studies of the human electroencephalogram: a review and a meta-analysis. Biol. Psychol. 61 (1–2), 111–138.
van Pelt, S., Boomsma, D.I., Fries, P., 2012. Magnetoencephalography in twins reveals a strong genetic determination of the peak frequency of visually induced γ-band synchronization. J. Neurosci. 32 (10), 3388–3392.
van Pelt, S., Shumskaya, E., Fries, P., 2018. Cortical volume and sex influence visual gamma. Neuroimage 178, 702–712.
van Soelen, I.L., Brouwer, R.M., van Baal, G.C., Schnack, H.G., Peper, J.S., Collins, D.L., Evans, A.C., Kahn, R.S., Boomsma, D.I., Hulshoff Pol, H.E., 2012. Genetic influences on thinning of the cerebral cortex during development. Neuroimage 59 (4), 3871–3880.
Van Veen, B.D., van Drongelen, W., Yuchtman, M., Suzuki, A., 1997. Localization of brain electrical activity via linearly constrained minimum variance spatial filtering. IEEE Trans. Biomed. Eng. 44 (9), 867–880.
Vidal, J.R., Chaumon, M., O`Regan, J.K., Tallon-Baudry, C., 2006. Visual grouping and the focusing of attention induce gamma-band oscillations at different frequencies in human magnetoencephalogram signals. J. Cogn. Neurosci. 18 (11), 1850–1862.
Werkle-Bergner, M., Shing, Y.L., Müller, V., Li, S.C., Lindenberger, U., 2009. EEG gamma-band synchronization in visual coding from childhood to old age: evidence from evoked power and inter-trial phase locking. Clin. Neurophysiol. 120 (7), 1291–1302.
Wierenga, L.M., Langen, M., Oranje, B., Durston, S., 2014. Unique developmental trajectories of cortical thickness and surface area. Neuroimage 87, 120–126.
Wiesman, A.I., Wilson, T.W., 2019. The impact of age and sex on the oscillatory dynamics of visuospatial processing. Neuroimage 185, 513–520.
Wiesman, A.I., Wilson, T.W., 2020. Attention modulates the gating of primary somatosensory oscillations. Neuroimage 211, 116610.
Wilson, T.W., Heinrichs-Graham, E., Proskovec, A.L., McDermott, T.J., 2016. Neuroimaging with magnetoencephalography: a dynamic view of brain pathophysiology. Transl. Res. 175, 17–36. https://doi.org/10.1016/j.trsl.2016.01.007.
Wilson, T.W., Slason, E., Asherin, R., Kronberg, E., Reite, M.L., Teale, P.D., Rojas, D.C., 2010. An extended motor network generates beta and gamma oscillatory perturbations during development. Brain Cogn. 73 (2), 75–84.